

Controlling Selectivity in Alkyl Oxidation with Oxygen Coverage: The Reactions of Ethyl and 2-Propyl Iodide on Oxygen-Covered Rh(111)

C. W. J. Bol and C. M. Friend*

Harvard University, Department of Chemistry, Cambridge, Massachusetts 02138

Received: March 17, 1995; In Final Form: May 19, 1995*

The oxidation of alkyl iodides on oxygen-covered Rh(111) has been studied using temperature-programmed reaction and high-resolution electron energy loss spectroscopies. Ethyl and 2-propyl iodide are selectively oxidized to acetaldehyde and acetone with selectivities of ~62% and ~40%, respectively, on Rh(111)-p(2 × 1)-O ($\theta_{\text{O}} = 0.5$). Formation of ethene and propene are competing pathways. No CO or CO₂ is formed at this oxygen coverage. C–I bond breakage in the intact alkyl iodides is proposed to be the rate-determining step in the formation of both the alkenes and the oxygenates. The resulting alkyl either rapidly dehydrogenates, eliminating the alkene, or adds oxygen, forming a transient alkoxy which subsequently eliminates the aldehyde or ketone via dehydrogenation. The selectivities for the different reaction pathways depend strongly on the oxygen coverage. On clean Rh(111), nonselective decomposition to H₂ and adsorbed carbon is the dominant pathway. At moderate oxygen coverages ($\theta_{\text{O}} < 0.3$), CO, CO₂, alkene, and alkane formation predominate. The strong dependence of the product distributions on the oxygen coverage is attributed to the multifunctional role of oxygen on Rh(111). Oxygen inhibits dehydrogenation such that selective β -H elimination and oxygen addition are enhanced at the expense of nonselective dehydrogenation leading to CO and CO₂. Carbon–iodine bond cleavage is also retarded by oxygen so that the resulting alkyl radical rapidly reacts to products at high oxygen coverage, allowing for direct oxygen addition to the alkyls. The strong dependence of product distribution on oxygen coverage has important implications for alkane oxidation on Rh catalysts and is in excellent agreement with recent studies of alkane oxidation over rhodium monoliths. Our results suggest that the oxygen coverage can be used to manipulate product distributions in alkane oxidation so as to enhance direct partial oxidation.

Introduction

Alcohols, aldehydes, and ketones are valuable building blocks in organic synthesis and are potential fuel alternatives. Currently, oxygenated hydrocarbons can be produced from natural gas in an energy-intensive two-step process, in which natural gas is converted to syngas (CO and H₂), from which oxygenated hydrocarbons are subsequently synthesized.¹ Direct, partial oxidation of alkanes would represent a great advance in fuel conversion and remains one of the great challenges in heterogeneous catalysis. Although these reactions are exothermic and should proceed readily on metal surfaces, high selectivities for partial oxidation are difficult to achieve, because total combustion of alkanes to CO₂ and H₂O is significantly more favorable thermodynamically. One possible solution that has been employed in some systems is to maintain a low partial pressure of oxygen; however, conversions are generally low under such conditions.² Ultrahigh-vacuum studies of oxidation reactions on transition-metal surfaces have shown that complete combustion is favored at high oxygen coverages on most metals,³ consistent with the trend of less combustion at low oxygen concentrations. Oxidation of olefins on Rh(111) is an exception to this trend; partial oxidation is enhanced at high oxygen coverages.^{4–7}

Recently, Schmidt et al. have shown that alkane combustion can be limited by using short contact times ($\sim 10^{-3}$ s) over Rh and Pt monolith catalysts, so that secondary oxidation of primary products is minimized.^{8–11} For example, CO and H₂ are the primary products of methane oxidation over Rh monoliths, accounting for 90% of the reaction. Likewise, ethane is oxidized mainly to CO and H₂ over the Rh monoliths; only 30% forms

ethylene.¹¹ Interestingly, the product distributions are significantly different for Pt and Rh monoliths, even though combustion is limited in both cases. In particular, the selectivity for ethylene formation from ethane is ~70% and for CO from methane only 60% on Pt. These differences are clearly the result of different relative rates for the competing pathways on the two metals. Schmidt et al. have pointed out the difference in the reactivity of surface oxygen on Pt and Rh;^{11,12} however, very little is known about the reactions of hydrocarbon intermediates, e.g., alkyls, important in these alkane oxidation processes. Herein, we specifically investigate competing reaction pathways, such as β -C–H bond cleavage to eliminate ethylene vs nonselective dehydrogenation and C–C bond breaking to yield CO, in ethyl. Alkane oxidation over Rh monoliths is particularly suitable for fundamental studies because the conditions of the experiment are similar to ultrahigh-vacuum studies: the monolith surface is relatively clean at steady state, and the short contact times lead to product distributions that are reflective of primary reaction products.

This investigation specifically addresses issues of reactivity important in alkane oxidation by using alkyl iodides as a source of alkyls. The study of alkyl reactivity is germane to alkane oxidation because the initial activation step is thought to be cleavage of a single C–H bond to form an alkyl.^{2,13} By investigating alkyls, the initial activation step, which is difficult under ultrahigh-vacuum conditions because the adsorption energy is low relative to the barrier for dehydrogenation, is circumvented and important mechanistic information is obtained. The reactivity of alkyls is also pertinent to testing the mechanism of 2-propyl thiolate reaction on oxygen-covered Rh(111).^{14,15} Previous studies have shown that the relatively weak C–I bond in a range of alkyl iodides selectively cleaves on a variety of

* Abstract published in *Advance ACS Abstracts*, July 1, 1995.

metal surfaces to produce alkyl intermediates.^{16–26} We have exploited this principal in this study in order to deliver ethyl and 2-propyl groups to the Rh(111) surface.

Fundamental studies of alkyl reactions as a function of oxygen coverage may suggest means for manipulating the product distributions in the catalytic system. We have previously shown that partial oxidation reactions on oxygen-covered Rh(111) are enhanced at high oxygen coverages. Combustion is favored at intermediate coverages and oxidation to CO at low oxygen concentrations.^{4–7,27} This is opposite the trend observed on other metals³ and is attributed to the fact that oxygen does not act as a Brønsted base on Rh(111). On many metal surfaces, oxygen promotes dehydrogenation reactions;³ conversely, oxygen inhibits C–H bond breaking on Rh(111). Accordingly, the oxygen coverage may be used to favor bond-selective chemistry in alkyls bound to oxygen-covered Rh(111) and would suggest that appropriate adjustment of the reaction conditions over the monoliths could lead to partial oxidation products, such as aldehydes, ketones, or organic acids. Indeed, we find that alkyl dehydrogenation is limited at high oxygen coverages on Rh(111) such that there is no detectable combustion or CO production. Instead, olefin elimination via β -C–H bond cleavage and acetaldehyde and acetone formation via alkoxide intermediates occur for ethyl and 2-propyl iodide, respectively.

Experimental Section

All experiments were performed in a stainless steel ultrahigh vacuum chamber with a base pressure of 1×10^{-10} Torr, which has been described in detail elsewhere.²⁸ Preparation and cleaning of the Rh(111) crystal,²⁹ as well as the preparation of the oxygen overlayers,¹⁵ have been described previously. The details of the experimental setup and procedures used can also be found elsewhere.¹⁵

In the temperature-programmed reaction experiment, the reactants are introduced to a freshly prepared surface at 100 K. The surface is subsequently heated to 700 K with the crystal face in line-of-sight of an apertured mass spectrometer (UTI-100C) that is computer controlled so as to monitor intensities of up to 10 masses vs time in a single experiment. The heating rate decreases monotonically from 9 K/s at 100 K to 6 K/s at 700 K and is highly reproducible. The crystal is negatively biased at -60 V to preclude any electron-induced chemistry.

In the high resolution electron energy loss experiments the reactants are introduced to the surface as described above. The surface is subsequently heated to the desired temperature at a rate approximately the same as in the temperature programmed reaction experiments and then allowed to cool to 100 K before recording a spectrum. All spectra reported were recorded at specular detection angles. The spectrometer (LK2000-14-R) operates at a primary beam energy of 3 eV, with a resolution of 55 cm^{-1} at a count rate of more than 1×10^6 counts/s for the elastic peak on the clean Rh(111) surface.

2-Propyl iodide (Aldrich, 99%) and ethyl iodide (Aldrich, 99%) were protected from light and subjected to several freeze–pump–thaw cycles before each dose. $^{16}\text{O}_2$ (Matheson, 99.99%) and $^{18}\text{O}_2$ (Cambridge Isotopes) were used as received. The purities of all samples were confirmed mass spectrometrically.

Results

Temperature-Programmed Reaction of 2-Propyl Iodide on Oxygen-Covered Rh(111). 2-Propyl iodide reacts via several competing channels on clean and oxygen-covered Rh(111) and the product distribution depends strongly on the initial oxygen coverage. Acetone, propene, and H_2O are the only reaction products, all evolving at 335 K, during the

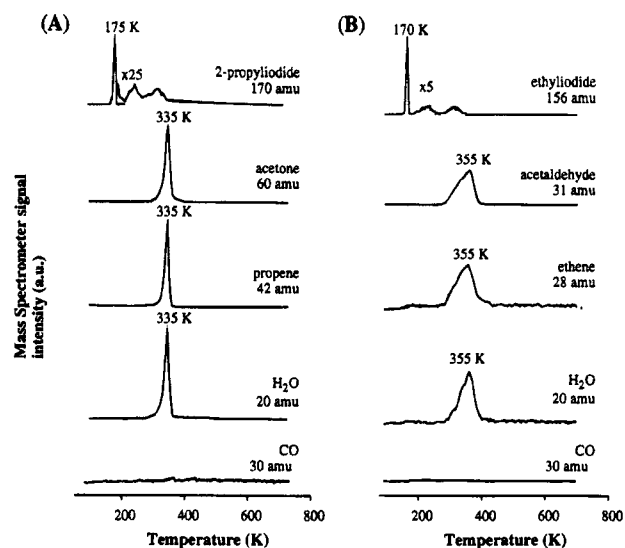


Figure 1. Temperature programmed reaction spectra of (A) 2-propyl iodide and (B) ethyl iodide on Rh(111)- $p(2 \times 1)-^{18}\text{O}$. The evolution of acetaldehyde is followed at 31 amu, rather than at the parent molecule, 46 amu, because oxidation of background CO can lead to intensity at 46 amu. All data are corrected for fragmentation from other products.

temperature-programmed reaction of 2-propyl iodide on Rh(111)- $p(2 \times 1)-\text{O}$, ($\theta_{\text{O}} = 0.5$ monolayers, Figure 1A). The acetone and propene peaks have essentially the same line shape, suggesting that they are formed from the same intermediate and via the same rate-limiting step. Condensed layers of 2-propyl iodide sublime at 175 K; molecular desorption continues up to 350 K. The remaining oxygen and iodine evolve at 1100 and 850 K, respectively. No other products, notably no CO or CO_2 , are detected in an extensive search from 2 to 170 amu for 2-propyl iodide reaction on Rh(111)- $p(2 \times 1)-\text{O}$.

Approximately 0.10 ± 0.01 ³⁰ molecules of 2-propyl iodide react per rhodium atom on Rh(111)- $p(2 \times 1)-\text{O}$, of which $40 \pm 12\%$ form acetone and $60 \pm 12\%$ propene. The acetone yield is estimated to be 0.04 ± 0.005 molecule/rhodium by comparing the integrated mass spectrometer signal to that of a known quantity of acetone formed in the reaction of 2-propanol on Rh(111)- $p(2 \times 1)-\text{O}$.²⁷ After reaction, 0.41 ± 0.02 monolayers of oxygen remain on the surface, based on a comparison of the integrated signal intensity of the O_2 desorption after reaction to that of the full $p(2 \times 1)-\text{O}$ overlayer. No carbon remains on the surface following reaction. The propene and water yields are estimated to be 0.06 ± 0.01 and 0.05 ± 0.01 per Rh atom, respectively, based on the amount of residual oxygen. Acetone and propene are the only hydrocarbon products on the $p(2 \times 1)-\text{O}$ overlayer, determining the total amount of 2-propyl iodide reacting at 0.10 ± 0.01 molecule/rhodium atom.

As the initial oxygen coverage is decreased, new products are formed (Figure 2) and the total amount of 2-propyl iodide that reacts increases monotonically. For example, the total amount of reaction is estimated to be 0.23 ± 0.02 monolayer on clean Rh(111), 0.13 ± 0.01 on Rh(111)- $p(2 \times 2)-\text{O}$ ($\theta_{\text{O}} = 0.25$ monolayer), and 0.10 ± 0.01 on Rh(111)- $p(2 \times 1)-\text{O}$ ($\theta_{\text{O}} = 0.5$ monolayer).³⁰ Carbon dioxide, H_2 and propane are observed for oxygen coverages below 0.35 and CO production is observed when the oxygen coverage decreases below 0.25 (Figure 2). Concomitantly, the acetone production diminishes to nearly zero when the initial oxygen coverage is 0.25 or lower. Propene is produced at all oxygen coverages, with the yield reaching a maximum of $70 \pm 7\%$ at an oxygen coverage of 0.35 monolayer. On the clean surface, nonselective decomposi-

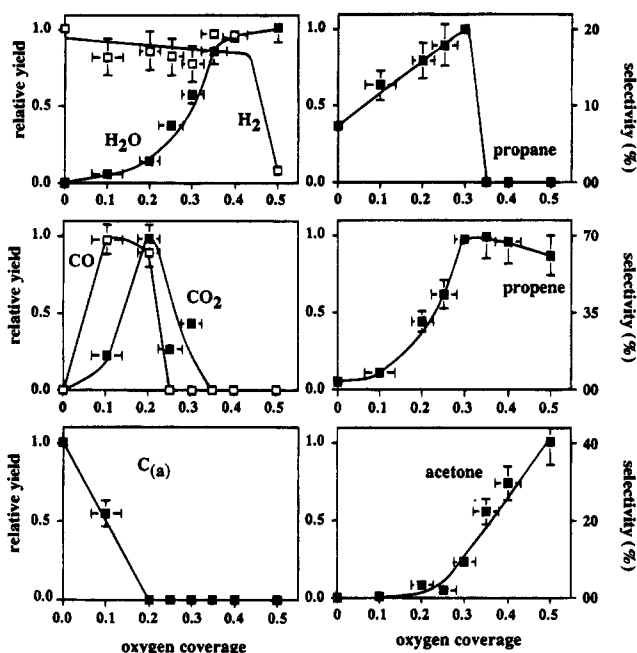


Figure 2. Relative yields of H_2 , H_2O , CO , CO_2 , adsorbed C , propene, propane, and acetone and selectivities for propene, propane, and acetone formation in the reaction of 2-propyl iodide on oxygen-covered $\text{Rh}(111)$ as a function of oxygen coverage. The yields are normalized for the total amount of 2-propyl iodide reacting.

tion to gaseous H_2 and surface carbon predominates; some propene and trace amounts of propane are also detected.

The yields of propene, acetone and water in the reaction of 2-propyl iodide on $\text{Rh}(111)$ with less than 0.5 monolayer of oxygen, are estimated by comparison to their respective yields on the $\text{p}(2 \times 1)\text{-O}$ overlayer. The propane yield is estimated based on the signal intensity at amu 43, compared to that of propene at amu 42, corrected for their relative mass spectrometer sensitivities. The yield of CO is determined by comparing the integrated signal intensity in its evolution to the desorption yield from $\text{Rh}(111)\text{-(}2 \times 2\text{)-}3\text{-CO}$, which is known to have a coverage of 0.75.³¹⁻³³ The CO_2 yield is estimated from its integrated signal intensity relative to that for CO oxidation on $\text{Rh}(111)\text{-p}(2 \times 1)\text{-O}$, where the residual oxygen concentration is used to determine the absolute yield. The total amount of 2-propyl iodide reacting on each specific surface is estimated based on the integrated signal intensity in the evolution of iodine around 850 K, using the iodine yield from the reaction of 2-propyl iodide on $\text{Rh}(111)\text{-p}(2 \times 1)\text{-O}$ as a standard.

The change in product distributions as a function of oxygen coverage, indicates that oxygen inhibits the nonselective breakdown of the hydrocarbon skeleton, leading to an increase in the yields of hydrocarbon products and a decrease in the amount of total decomposition.³⁴ Above 0.20 monolayer of oxygen no $\text{C}_{(a)}$ is formed, and above 0.35 monolayer no evolution of CO and CO_2 is observed either. At relatively low initial oxygen coverages, $\theta_{\text{O}} = 0.1\text{--}0.2$, $\text{C}_{(a)}$, CO and H_2 are the primary products, whereas propene, CO_2 , H_2 , and H_2O are the most abundant products at moderate oxygen coverages, $\theta_{\text{O}} = 0.2\text{--}0.35$ (Figure 2). For example, of the 0.13 ± 0.01 molecules of 2-propyl iodide that react on $\text{Rh}(111)\text{-p}(2 \times 2)\text{-O}$ ($\theta_{\text{O}} = 0.25$), 0.067 ± 0.010 form propene, 0.018 ± 0.003 propane, and 0.009 ± 0.001 acetone, while the remainder is completely oxidized yielding 0.108 ± 0.011 molecules of CO_2 . H_2O (0.029 ± 0.004 molecules) and H_2 (0.063 ± 0.009 molecules) are also formed. The propane yield is a maximum for an oxygen coverage of 0.2 monolayer. Propane formation requires a combination of hydrogenation and dehydrogenation of 2-propyl iodide and,

therefore, is a maximum for intermediate oxygen coverages; the dehydrogenation is the source of hydrogen for the hydrogenation.

The products from 2-propyl iodide reaction are unambiguously identified on the basis of the measured fragmentation pattern. Acetone, propene, and water are the only products of reaction on $\text{Rh}(111)\text{-p}(2 \times 1)\text{-O}$ (Table 1). The highest masses observed are 58 amu for reaction on ^{16}O -covered $\text{Rh}(111)$ and 60 amu for reaction on ^{18}O -covered $\text{Rh}(111)$, as illustrated for $\text{Rh}(111)\text{-p}(2 \times 1)\text{-O}$ (Table 1). These data and the observed shift in intensity from 43 to 45 amu upon reaction on the ^{18}O -labeled overlayer demonstrate that the product has the molecular formula $\text{C}_3\text{H}_6\text{O}$. All possible products with this stoichiometry, except acetone, can be excluded on the basis of their fragmentation patterns (Table 1). Furthermore, the ratio of 43:58 amu, the two major fragments of acetone, is the same in the product peak at 335 K as that measured for an authentic acetone sample, within experimental error. The fragmentation pattern of the products evolving from $\text{Rh}(111)\text{-p}(2 \times 1)\text{-O}$ at 375 K cannot be accounted for by acetone alone, however. For example, the 41 and 42 amu intensities are substantially higher than for acetone and do not change upon reaction on the ^{18}O -labeled overlayer, indicating the concomitant formation of a hydrocarbon. The residual ion-intensity distribution of the product, following subtraction of the ketone spectrum, closely resembles that of propene (Table 1), identifying it as a second product. A similar protocol was used to identify propene for lower oxygen coverages. Propane formation is identified by the signal intensity at 43 amu in the reaction on the ^{18}O -labeled surface. Water formation is identified by signal intensity at 18 and 20 amu for reaction on ^{16}O - and ^{18}O -labeled $\text{Rh}(111)$, respectively. H_2 , CO , and CO_2 evolve in peaks with different maxima and line shapes and are easily distinguished from the other products.

Temperature-Programmed Reactions of Ethyl Iodide on Oxygen-Covered $\text{Rh}(111)$. The reactions of ethyl iodide are qualitatively similar to those of 2-propyl iodide in that analogous products are formed and the dependence of the product distribution on initial oxygen coverage is similar. There are two important quantitative differences in the ethyl vs 2-propyl reactions: the total amount of ethyl iodide that reacts is less, and the peak temperature for product formation on $\text{Rh}(111)\text{-p}(2 \times 1)\text{-O}$ is higher for the ethyl iodide reaction. These two differences are proposed to arise from the difference in their C-I bond strengths: 55.3 and 54.3 kcal/mol for ethyl and 2-propyl iodide, respectively.³⁵

Acetaldehyde, ethene, and H_2O are formed at 355 K during temperature programmed reaction of ethyl iodide on $\text{Rh}(111)\text{-p}(2 \times 1)\text{-O}$ (Figure 1B). Again, no CO or CO_2 are formed at this oxygen coverage. Condensed multilayers of ethyl iodide sublime at 170 K, and molecular desorption competes with reaction up to 350 K. Deposited iodine and the remaining oxygen desorb around 850 and 1100 K, respectively. Acetaldehyde and propene evolve with indistinguishable line shapes at 355 K on $\text{Rh}(111)\text{-p}(2 \times 1)\text{-O}$, suggesting identical kinetics in their formation. Notably, these spectra are similar to the acetone and propene evolution peaks from 2-propyl iodide (Figure 1A). Water is also formed from ethyl iodide reaction on $\text{Rh}(111)\text{-p}(2 \times 1)\text{-O}$ with very similar kinetics, differing only in the leading edge. The evolution of the products is limited by their formation, since molecular acetaldehyde, ethene, and H_2O desorb from $\text{Rh}(111)\text{-p}(2 \times 1)\text{-O}$ at 245,³⁶ 215,³⁶ and 185 K,³⁷ respectively.

Approximately 0.05 ± 0.01 molecules of ethyl iodide react per rhodium atom on $\text{Rh}(111)\text{-p}(2 \times 1)\text{-O}$, based on com-

TABLE 1: Fragmentation Patterns of the Reaction Products of 2-Propyl Iodide on Rh(111)-p(2 × 1)-O

molecule	intensity at <i>m/e</i>											
	15	27	28	29	31	41	42	43	45	57	58	170
acetone ^a	59	12	17	3		3	16	100			10	
2-propanol ^a	35	30	8	22	5	12	7	42	100		2	
2-propyl iodide ^a	8	54	7	3		53	10	100				5
propene ^a	6	53	27			100	57					
propane ^a	7	46	100	90		10	2	17				
propanal ^b		35	63	100		1	1	2		16	65	
propeneoxide ^b		63	100	68	30	1	3	33		2	43	
allyl alcohol ^b		20	12	40	30	7	1	1		100	27	
methyl vinyl ether ^b					55			63			100	
oxetane ^b		20	100	19	7	1	1	1		8	60	
¹⁶ O product	29	55	35			100	58	42			4	
¹⁶ O product (acetone spectrum scaled to amu 58 signal)	5	51	29	-1		100	52	2				

^a Measured in our laboratory spectrometer. ^b Taken from literature.⁴⁷

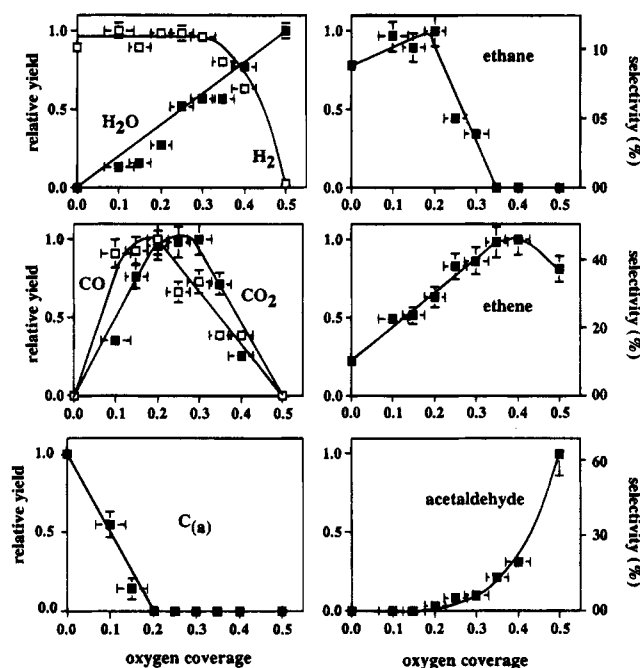


Figure 3. Relative yields of H₂, H₂O, CO, CO₂, adsorbed C, ethene, ethane, and acetaldehyde and selectivities for ethene, ethane, and acetaldehyde formation in the reaction of ethyl iodide on oxygen-covered Rh(111) as a function of the oxygen coverage. The yields are normalized for the total amount of ethyl iodide reacting.

parison of the integrated signal intensity in the iodine desorption around 850 K to that in the reaction of a saturation coverage of 2-propyl iodide on Rh(111)-p(2 × 1)-O. The selectivity for acetaldehyde production is estimated to be 62 ± 28%, while the remaining 38 ± 28% forms ethene on the p(2 × 1)-O surface. These selectivities are derived from the saturation coverage of ethyl iodide and the total amount of water formed in the reaction, determined to be 0.028 ± 0.002 molecules/rhodium by comparison to the water yield in the reaction of 2-propyl iodide on Rh(111)-p(2 × 1)-O.

As for the 2-propyl iodide, the total amount of ethyl iodide reaction and the product distributions depend strongly on the initial oxygen coverage (Figure 3). Specifically, the total amount of reaction decreases monotonically as a function of the oxygen coverage, from 0.46 ± 0.09 on clean Rh(111), to 0.18 ± 0.04 on Rh(111)-p(2 × 2)-O ($\theta_{\text{O}} = 0.25$) and 0.05 ± 0.01 on Rh(111)-p(2 × 1)-O ($\theta_{\text{O}} = 0.5$). Again, the amount of nonselective decomposition decreases with increasing oxygen coverage. For example, ethane formation is at a maximum at 0.20 monolayer of oxygen and ethene at 0.40 in the reactions

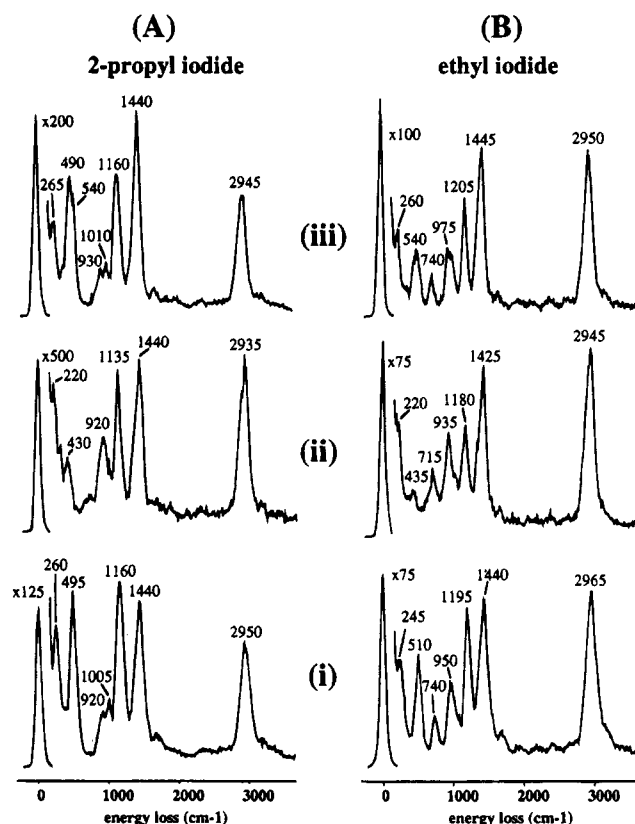


Figure 4. High-resolution electron energy loss spectra of (A) 2-propyl iodide and (B) ethyl iodide, corresponding to (i) condensed multilayers on Rh(111)-p(2 × 1)-¹⁸O at 100 K, (ii) monolayer on clean Rh(111) at 100 K, and (iii) monolayer on Rh(111)-p(2 × 1)-¹⁸O annealed at 250 K.

of ethyl iodide on oxygen-covered Rh(111). Acetaldehyde is observed for oxygen coverages above 0.20 monolayers; its yield increases sharply with increasing oxygen coverage up to the maximum attainable oxygen coverage, 0.50. The only significant difference between the ethyl and 2-propyl reactions is that CO and CO₂ production fall gradually over the range of 0.2–0.5 monolayers of oxygen in the case of ethyl iodide (Figure 3), whereas they fall off rapidly for the 2-propyl case (Figure 2). As for 2-propyl iodide no carbon is deposited during the reaction for oxygen coverage above 0.20 monolayers.

The yields of ethene, acetaldehyde, and water in the reaction of ethyl iodide on Rh(111) with less than 0.5 monolayers of oxygen are determined by comparison to their respective yields on the p(2 × 1)-O overlayer. The ethane yield is estimated based on the signal intensity at 29 amu, compared to ethene at

TABLE 2: Vibrational Assignments for 2-Propyl Iodide^a

	condensed multilayers on Rh(111)-p(2 × 1)- ¹⁸ O (100 K)	monolayer on Rh(111)-p(2 × 1)- ¹⁸ O (250 K)	monolayer on Rh(111) (100 K)	reference infrared data
$\nu(\text{Rh-I})$			220	
$\delta(\text{C-C-I})$	260	265		269
$\nu(\text{Rh-C})$			430	
$\nu(\text{C-I})$	495	490		499
$\nu(\text{Rh-}^{18}\text{O})$	nr	540		
$\rho(\text{CH}_3)/\nu(\text{C-C})$	920	930	920	925/879
$\rho(\text{CH}_3)$	1005	1010	nr	1020
$\rho(\text{CH}_3)$	1160	1160	1135	1153
$\delta(\text{CH}_3)$	1440	1440	1440	1459
$\nu(\text{C-H})$	2950	2945	2935	2978

^a Assignments are based on comparison to reference infrared data.³⁸

TABLE 3: Vibrational Assignments for Ethyl Iodide^a

	condensed multilayers on Rh(111)-p(2 × 1)- ¹⁸ O (100 K)	monolayer on Rh(111)-p(2 × 1)- ¹⁸ O (250 K)	monolayer on Rh(111) (100 K)	infrared data gas phase
$\nu(\text{Rh-I})$			220	
$\delta(\text{C-C-I})$	245	260		
$\nu(\text{Rh-C})$			435	
$\nu(\text{C-I})$	510	nr		496
$\nu(\text{Rh-}^{18}\text{O})$	nr	540		
$\rho(\text{CH}_2)$	740	740	715	736
$\nu(\text{C-C})$	950	975	935	949
$\omega(\text{CH}_2)$	1195	1205	1180	1199
$\delta(\text{CH}_3)$	1440	1445	1425	1452
$\nu(\text{C-H})$	2965	2950	2945	2968

^a Assignments are based on comparison to gas-phase infrared data.⁴⁸

28 amu, corrected for their respective mass spectrometer sensitivities. CO and CO₂ yields are determined as described above for 2-propyl iodide.

The products were identified mass spectrometrically using a similar procedure as described for 2-propyl iodide. Acetaldehyde is identified on the basis of intensity at 29, 43, and 44 amu for the reaction on ¹⁶O-labeled Rh(111), and 31, 45, and 46 amu for the reaction on ¹⁸O-labeled Rh(111). Oxirane, the only other possible product with stoichiometry C₂H₄O, can be ruled out based on the lack of signal at 15 amu. Ethene is identified on the basis of intensity at 26, 27, and 28 amu, after subtraction of the ion intensity due to the evolution of ethyl iodide, scaled to its intensity at 156 amu. Ethane is identified by signal intensity at 29 and 30 amu. The evolution of CO, CO₂ and H₂ is followed at 28, 44, and 2 amu and 30, 48, and 2 amu for reaction on ¹⁶O-labeled and ¹⁸O-labeled overlayers, respectively.

High Resolution Electron Energy Loss Experiments. 2-Propyl iodide remains intact up to the onset of product formation on Rh(111)-p(2 × 1)-O based on high resolution electron energy loss data (Figure 4A, Table 2). The spectrum recorded after heating a saturated layer of 2-propyl iodide to 250 K is virtually identical to that of the condensed molecule. All modes, including the modes associated with an intact C-I bond, $\delta(\text{C-C-I})$ at 260 cm⁻¹ and $\nu(\text{C-I})$ at 295 cm⁻¹, are still present. The assignments of the modes are made based on comparison to reference infrared data (Table 2).³⁸

The temperature required for C-I bond breakage increases with increasing oxygen coverage. The C-I bond cleaves upon adsorption at 100 K on clean Rh(111) (Figure 4Aii). The absence of the modes associated with intact C-I bonds, $\delta(\text{C-C-I})$ at 260 cm⁻¹ and $\nu(\text{C-I})$ at 295 cm⁻¹, and the presence of modes at 220 cm⁻¹, $\nu(\text{Rh-I})$, and 430 cm⁻¹, $\nu(\text{Rh-C})$, are a clear indication of C-I bond breakage, affording adsorbed 2-propyl and iodine. On Rh(111)-p(2 × 2)-O ($\theta_{\text{O}} = 0.25$; data not shown), the C-I bond stays intact up to 215 K and on

Rh(111)-p(2 × 1)-O ($\theta_{\text{O}} = 0.5$) until 265 K (Figure 4), the onset of reaction. The vibrational spectra are similar for the p(2 × 2)-O and p(2 × 1)-O surfaces at 100 K.

Ethyl iodide also remains intact on Rh(111)-p(2 × 1)-O up to its reaction temperature (Figure 4B, Table 3). The high resolution electron energy loss spectrum of a saturated layer of ethyl iodide ($\theta = 0.05$) annealed to 250 K is essentially identical to that of condensed ethyl iodide. The presence of the loss at 260 cm⁻¹, assigned to the $\delta(\text{C-C-I})$, is indicative of intact C-I bonds. The loss, due to the $\nu(\text{C-I})$, expected around 510 cm⁻¹, is obscured by the $\nu(\text{Rh-}^{18}\text{O})$ at 540 cm⁻¹. The temperature required for C-I bond breakage in ethyl iodide also increases as a function of increasing oxygen coverage. Analogous to 2-propyl iodide the C-I bond in ethyl iodide is cleaved upon adsorption at 100 K on clean Rh(111), affording adsorbed ethyl and iodine, based on the absence of the $\delta(\text{C-C-I})$ and $\nu(\text{C-I})$ modes and the presence of modes at 220 cm⁻¹, $\nu(\text{Rh-I})$, and 430 cm⁻¹, $\nu(\text{Rh-C})$, in the corresponding spectrum (Figure 4Bii). The resulting spectrum is in good agreement with earlier reported spectra of ethyl adsorbed on Pt(111)³⁹ and Cu(111).⁴⁰ On Rh(111)-p(2 × 2)-O, C-I bond breakage is first observed at 225 K, the onset of product evolution on this surface. As for 2-propyl iodide, the vibrational spectra obtained for ethyl iodide on Rh(111)-p(2 × 1)-O is similar to that for Rh(111)-p(2 × 2)-O (data not shown). Finally, the C-I bond stays intact up to 275 K on Rh(111)-p(2 × 1)-O, just below the temperature of product evolution.

Discussion

Both ethyl and 2-propyl iodide are proposed to react via their respective radicals on Rh(111)-p(2 × 1)-O (Figure 5). On oxygen-covered Rh(111), oxygen addition to the radicals would yield the corresponding alkoxides which rapidly react to produce the aldehyde (ketone). 2-Propoxy²⁷ and ethoxy,³⁶ formed from their respective alcohols, are known to undergo β -hydrogen

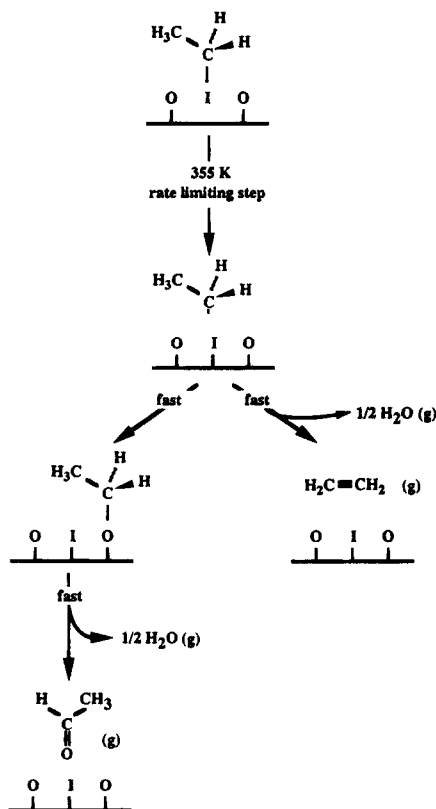


Figure 5. Schematic of proposed mechanism for the oxidation of ethyl iodide on Rh(111)-p(2 × 1)-O.

elimination to acetone and acetaldehyde, respectively, at 265 K on Rh(111)-p(2 × 1)-O; hence, 2-propoxy and ethoxy would rapidly eliminate acetone and acetaldehyde at temperatures above 300 K, once formed from oxygen addition to the respective alkyl radicals. Olefin elimination via dehydrogenation of the ethyl and 2-propyl radicals, or their respective surface alkyls, is a competing reaction on Rh(111)-p(2 × 1)-O. β -H elimination from alkyls is well-known on other metal surfaces^{20,41-43} and in organometallic complexes.⁴⁴

All of our data indicate that the radicals rapidly react via one of these pathways as the C-I bond breaks on Rh(111)-p(2 × 1)-O. First of all, the identical line shape in the evolution of carbon-containing products from Rh(111)-p(2 × 1)-O, e.g., ethene and acetaldehyde in the reaction of ethyl iodide and propene and acetone in the reaction of 2-propyl iodide, strongly suggests that they are formed from a single intermediate with the same rate-determining step. Second, both ethyl iodide and 2-propyl iodide remain intact up to the onset of product evolution from Rh(111)-p(2 × 1)-O, as shown by high-resolution electron energy loss data. Furthermore, the relative temperatures required for product evolution correlate with the C-I bond strengths in the free alkyl iodides, indicating that C-I bond breaking determines the rate of reaction. The gas-phase C-I bond strengths for ethyl iodide and 2-propyl iodide are 55.3 and 54.3 kcal/mol,³⁵ respectively, compared to a reaction temperature of 355 K for ethyl iodide and 335 K for 2-propyl iodide, corresponding to approximate activation energies of 21 and 20 kcal/mol, assuming a preexponential factor of 10^{13} s^{-1} .⁴⁵ Indeed, the proposed mechanism is supported by preliminary studies of the reactions of gaseous methyl radicals with clean Rh(111) and Rh(111)-p(2 × 1)-O.⁴⁶ Vibrational spectroscopy shows that methoxy is formed by direct addition of gaseous methyl radicals to surface oxygen at 100 K and not by the reaction of surface methyl and oxygen. Furthermore, radical formation has previously been reported in the reaction of alkyl iodides on Cu(111).²²⁻²⁶

Other possible mechanisms can be excluded based on our data. Formation of acetone could potentially proceed through propene; similarly, acetaldehyde could be produced via ethene oxidation. Although acetone formation has been observed in the reaction of propene on Rh(111)-p(2 × 1)-O,⁷ the acetone yield from propene oxidation is too small to account for the observed acetone formation in the reaction of 2-propyl iodide. No acetaldehyde is observed in the reaction of ethene on Rh(111)-p(2 × 1)-O.³⁶ A mechanism involving concerted C-I bond cleavage and C-O bond formation can also be excluded, since 2-propoxide formed from 2-propanol on oxygen-covered Rh(111) reacts with complete retention of the C-O bond.²⁷ Therefore, there would be no olefin production in such a mechanism.

Most striking is the unusual dependence in the product distributions as a function of oxygen coverage. Specifically, the more fully oxidized products, CO and CO₂, are formed at low-to-intermediate oxygen coverages, whereas the partial oxidation products, acetaldehyde and acetone, are formed at high oxygen coverages. While a detailed mechanism cannot be formulated for oxygen coverages below 0.5 because of the complexity of the reactions, it is clear that oxygen adsorbed on Rh(111) inhibits dehydrogenation and C-I bond breaking. The inhibition of dehydrogenation at high oxygen coverages explains the decrease in the fraction of the alkyls that react to CO and CO₂ as the oxygen coverage is increased above 0.25 monolayer. At low oxygen coverages, there are ample free Rh sites that induce C-H bond breaking; subsequent oxidation by surface oxygen leads to CO and CO₂. The predominance of CO production at low oxygen coverages is attributed to a statistical effect; at lower oxygen coverages, CO production will dominate from the C + O reaction. The increase in the selectivity for CO₂ vs CO production up to ~0.3 monolayer is consistent with an increase in the probability of carbon reaction with two oxygens on the surface. Ultimately, at initial oxygen coverages of ~0.25, the inhibition of dehydrogenation leads to a change in mechanism so that acetone and acetaldehyde are produced via the mechanism outlined in detail for Rh(111)-p(2 × 1)-O (Figure 5). The increase in the olefin production can be similarly rationalized. The inhibition of nonselective dehydrogenation by oxygen leads to selective β -H elimination from the alkyl to afford the corresponding olefin. The alkane yields represent a balance between the hydrogenation and dehydrogenation pathways in that dehydrogenation supplies the hydrogen necessary to produce alkanes from hydrogenation of the intact alkyls. The unusual manner in which oxygen influences selectivities on Rh(111) is attributed to the fact that oxygen on Rh(111) does not act as a Brønsted base but in fact inhibits C-H bond breakage by the surface.⁷

The inhibition in combustion at high oxygen coverages has important implications for alkane oxidation catalysis by Rh and is the opposite trend reported for other transition-metal surfaces, supported catalysts, and metal oxides. Generally, the selectivity for combustion products increases as the oxygen coverage (partial pressure) is increased in methane oxidation.^{2,3,13} Our results suggest that high steady-state oxygen coverages would lead to enhanced production of ethylene and acetaldehyde in the oxidation of ethane over Rh, for example, as long as the reaction proceeds under single-collision conditions. Alkyl radicals are generally thought to be the key intermediates in alkane oxidation; hence, these studies have a direct bearing on the mechanism of ethane and propane oxidation by Rh. Notably, our results are in good agreement with selectivities measured for ethane oxidation over Rh monolith catalysts under conditions where the contact times are short. In particular, CO

and H₂ are formed with 70% selectivity,¹¹ compared to 55% selectivity for an initial oxygen coverage of 0.1 monolayer.

The potential role of iodine in the observed trends still needs to be fully addressed. Iodine has been used to enhance the production of formaldehyde from methane oxidation on Pd catalysts, for example.² Furthermore, dissociation of the C–I bond in both ethyl and 2-propyl iodide are inhibited by surface oxygen. While this is not surprising, because of steric considerations, it does raise the issue of what role iodine plays in the reaction since this effect leads to a decrease in the iodine coverage as the initial oxygen coverage is increased. We do not think that the iodine plays a significant role in determining the inhibition of dehydrogenation as a function of increasing oxygen coverage because a similar trend has been observed for olefins,^{4–7} alkoxides,²⁷ and 2-propyl thiolate.^{14,15} Indeed, the reactions of 2-propyl thiolate on oxygen-covered Rh(111) are very similar to those of 2-propyl iodide, indicating that both react via a radical mechanism. We plan to investigate the reactions of gaseous radicals, such as ethyl and methyl, with oxygen-covered Rh(111) to specifically test for the effect of coadsorbed iodine.

Conclusion

2-Propyl iodide and ethyl iodide react via similar pathways on clean and oxygen-covered Rh(111). Both molecules react to deliver their respective alkyls to the surface. On Rh(111)–p(2 × 1)–O, the barrier for C–I bond breaking limits the rate of reaction. The resulting alkyl radicals rapidly react to eliminate an olefin via β-H elimination or via competing oxygen addition to afford an alkoxide which rapidly yields acetone and acetaldehyde from 2-propyl and ethyl reaction, respectively.

The product distributions depend strongly on the oxygen coverage. The changes in the product distributions with oxygen coverage, while different than other metals, are consistent with inhibition of C–H bond breakage by oxygen on Rh(111). Accordingly, high oxygen coverages favor aldehyde (ketone) production both by increasing the probability of alkoxide formation and by increasing the selectivity for β-hydrogen elimination in the alkoxide once formed. The reported oxygen coverage dependence has important implications for catalytic alkane oxidation in that an increase in the steady-state oxygen coverage could lead to enhanced olefin elimination or partial oxidation.

Acknowledgment. We gratefully acknowledge the support of the National Science Foundation under Grant CHE-9421615.

References and Notes

- (1) *Catalysis in C₁ Chemistry*; Keim, W., Ed.; *Catalysis by Metal Complexes*; D. Reidel Publishing Company: Dordrecht, Holland, 1983.
- (2) Pitchai, R.; Klier, K. *Catal. Rev.-Sci. Eng.* **1986**, *28*, 13.
- (3) Madix, R. J.; Roberts, J. T. The problem of heterogeneously catalyzed partial oxidation: model studies on single crystal surfaces. In *Surface Reactions*, Madix, R. J., Ed.; Springer-Verlag: Berlin, 1994; p 5.

- (4) Xu, X.; Friend, C. M. *J. Am. Chem. Soc.* **1990**, *112*, 4571.
- (5) Xu, X.; Friend, C. M. *J. Phys. Chem.* **1991**, *95*, 10753.
- (6) Xu, X.; Friend, C. M. *J. Am. Chem. Soc.* **1991**, *113*, 8572.
- (7) Xu, X.; Friend, C. M. *J. Am. Chem. Soc.* **1991**, *113*, 6779.
- (8) Hickman, D. A.; Hauptfear, E. A.; Schmidt, L. D. *Catal. Lett.* **1993**, *17*, 223.
- (9) Torniaainen, P. M.; Chu, X.; Schmidt, L. D. *J. Catal.* **1994**, *146*, 1.
- (10) Huff, M.; Schmidt, L. D. *J. Catal.* **1994**, *149*, 127.
- (11) Huff, M.; Schmidt, L. D. *J. Phys. Chem.* **1993**, *97*, 11815.
- (12) Wagner, M. L.; Schmidt, L. D. *J. Phys. Chem.* **1995**, *99*, 805.
- (13) Gesser, H. D.; Hunter, N. R.; Prakash, C. B. *Chem. Rev.* **1985**, *85*, 235.
- (14) Bol, C. W. J.; Friend, C. M. *Surf. Sci. Lett.*, **1995**, *322*, L271–L274.
- (15) Bol, C. W. J.; Friend, C. M. *J. Am. Chem. Soc.* **1995**, *117*, 5351.
- (16) Jenks, C. J.; Bent, B. E.; Bernstein, N.; Zaera, F. *J. Am. Chem. Soc.* **1993**, *115*, 308.
- (17) Zaera, F. *Acc. Chem. Res.* **1992**, *25*, 260.
- (18) Tjandra, S.; Zaera, F. *Langmuir* **1993**, *10*, 2640.
- (19) Zhou, X.-L.; White, J. M. *J. Phys. Chem.* **1991**, *95*, 5575.
- (20) Tjandra, S.; Zaera, F. *Surf. Sci.* **1993**, *289*, 255.
- (21) Zaera, F. *Surf. Sci.* **1989**, *219*, 453.
- (22) Lin, J.-L.; Bent, B. E. *J. Phys. Chem.* **1993**, *97*, 9713.
- (23) Lin, J.; Bent, B. E. *J. Am. Chem. Soc.* **1993**, *115*, 6943.
- (24) Lin, J.; Bent, B. E. *J. Am. Chem. Soc.* **1993**, *115*, 2849.
- (25) Xi, M.; Bent, B. E. *Langmuir* **1994**, *10*, 505.
- (26) Xi, M.; Bent, B. E. *J. Am. Chem. Soc.* **1993**, *115*, 7426.
- (27) Xu, X.; Friend, C. M. *Surf. Sci.* **1992**, *260*, 14.
- (28) Ph.D. Thesis: Model Studies of Desulfurization Reactions on Mo(110); Wiegand, B. C. Harvard University: Cambridge, 1991.
- (29) Xu, X.; Friend, C. M. *J. Phys. Chem.* **1989**, *93*, 8072.
- (30) The errors are based on the standard deviation in the integrated mass spectrometer intensities in sets of five identical temperature-programmed reaction experiments. The signal intensities are highly reproducible, with standard deviation below 10%, but quoted errors are sometimes large due to propagation of errors in calculations.
- (31) Thiel, P. A.; Williams, E. D.; Yates, J. T. J.; Weinberg, W. H. *Surf. Sci.* **1979**, *84*, 54.
- (32) Van Hove, M. A.; Koestner, R. J.; Frost, J. C.; Somorjai, G. A. *Surf. Sci.* **1983**, *129*, 482.
- (33) VanHove, M. A.; Koestner, R. J.; Somorjai, G. A. *Phys. Rev. Lett.* **1983**, *50*, 903.
- (34) Total decomposition is defined as the complete breakdown of the hydrocarbon skeleton, yielding C_(s), CO, CO₂, H₂, and H₂O.
- (35) Griller, D.; Kanabus-Kaminska, J. M.; MacColl, A. *J. Mol. Struct.* **1988**, *163*, 125.
- (36) Bol, C. W. J.; Friend, C. M., unpublished data.
- (37) Wagner, F. T.; Moylan, T. E. *Surf. Sci.* **1987**, *191*, 121.
- (38) Klaboe, P. *Spectrochim. Acta* **1970**, *26A*, 87.
- (39) Lloyd, K. G.; Champion, A.; White, J. M. *Catal. Lett.* **1989**, *2*, 105.
- (40) Lin, J.; Bent, B. E. *J. Phys. Chem.* **1992**, *96*, 8529.
- (41) Jenks, C. J.; Chiang, C.; Bent, B. E. *J. Am. Chem. Soc.* **1991**, *113*, 6308.
- (42) Zaera, F. *J. Am. Chem. Soc.* **1989**, *111*, 8744.
- (43) Bent, B. E.; Nuzzo, R. G.; Zegarski, B. R.; Dubois, L. H. *J. Am. Chem. Soc.* **1991**, *113*, 1137.
- (44) See, for instance: (a) Burk, M. J.; McGrath, M. P.; Crabtree, R. H. *J. Am. Chem. Soc.* **1988**, *110*, 620. (b) Cree-Uchiyama, M.; Shapley, J. R.; St. George, G. M. *J. Am. Chem. Soc.* **1986**, *108*, 1316–1317. (c) Schrock, R. R.; Parshall, G. W. *Chem. Rev.* **1976**, *76*, 243–268.
- (45) Redhead, P. A. *Vacuum* **1962**, *12*, 203.
- (46) Bol, C. W. J.; Friend, C. M.; *J. Am. Chem. Soc.*, in press.
- (47) *EPA/NIH Mass Spectral Data Base*; Heller, S. R.; Milne, G. W. A., U. S. Government Printing Office: Washington, DC, 1978; Vol. 1.
- (48) Durig, J. R.; Thompson, J. W.; Thyagesan, V. W.; Witt, J. D. *J. Mol. Struct.* **1975**, *24*, 41.